A Relay Discharged FICDM Method for Improved Repeatability

Matthew Drallmeier (1), Lena Zeitlhoefler (2), Huiping Yang (3), Wei Huang (1), Friedrich zur Nieden (4), David Pommerenke (5)

(1) ESDEMC Technology LLC, 2001 Forum Drive, Rolla, MO 65401 USA
tel.: 573-202-6411, fax: 877-641-9358, e-mail: info@esdemc.com

(2) Technische Universität München, Arcisstr. 21, 80333 Munich, Germany
tel.: + 49 89 234 36529, e-mail: lena.zeitlhoefler@tum.de

(3) South China Normal University, Guangzhou, P.R. China
e-mail: huipingyang05@scnu.edu.cn

(4) Infineon Technologies AG, Am Campeon 1-15, 85579 Munich, Germany
Tel.: +49 89 234 21456, e-mail: friedrich.zurnieden@infineon.com

(5) Graz University of Technology, Inffeldgasse 12, 8010 Graz, Austria
e-mail: david.pommerenke@tugraz.at

Abstract – A new design for CDM testing is proposed that retains the field charging DUT method while providing a consistent discharge inside of a reed switch. The method is shown to adhere to the current JS-002 standard and to perform at low voltages, but JS-002 failures could not be exactly replicated.

I. Introduction

A CDM event occurs when the pin of a charged device approaches an external metal object such that the potential difference exceeds the breakdown voltage of the air gap between them. The device generally becomes charged by either E-field charging, in which electric fields near the device cause the potential of the device to change without changing its net charge, or Tribo-charging, in which a static charge is generated when the device slides on another surface [1]. The field induced CDM method (FICDM) is one of the best methods to simulate a true CDM event. In this method, the device is placed on a dielectric sheet, under which a plate of varying voltage levels changes the potential of the device, thereby emulating the E-field charging method. However, current FICDM testers are plagued with repeatability issues due to the variable spark resistance of the air discharge making the practice difficult to standardize [1][2]. As CDM testing voltages decrease, the variability of the air discharge increases, causing concern over the ability to meaningfully classify devices at lower voltages [3]. This is becoming increasingly problematic as the necessity for classification at lower levels is becoming greater with advances in IC technology [1].

This work presents a CDM tester that incorporates a relay into the pogo pin structure and maintains adherence to the Joint CDM Standard ANSI/ESDA/JEDEC JS-002 [2] for FICDM testing. The use of a mercury wetted reed switch in the pogo pin allows for a more consistent spark resistance during low voltage pulses when compared to discharges in air. The method also preserves the field induced charging method which closely replicates the real world CDM charging mechanism. This method may produce failures that cannot be exactly replicated by other contact first CDM testers [4]. The new CDM tester is evaluated in comparison to a standard FICDM system through discharge waveform comparisons on calibration modules and device failure analysis.

II. RP-CCDM Tester

A. Discharge Circuit

The RP-CCDM [5], or Relay Pogo-Contact First CDM, is a design of the CDM discharge head that allows for the use of a repeatable relay discharge while largely preserving the design parameters of the JS-002 standard. Figure 1 shows a cross section of the RP-CCDM head.

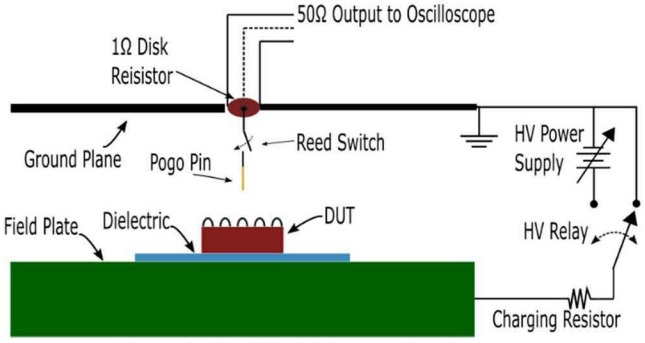

Figure 1: RP-CCDM System Configuration

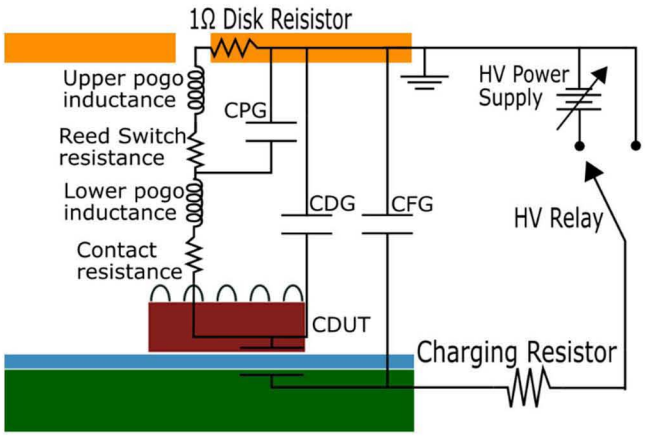

Figure 2: RP-CCDM Discharge Circuit

As shown in Figures 1 and 2, the RP-CCDM uses the field charging method as well as a similar discharge path to the one specified in the JS-002 standard. To charge the device, the pogo pin of the RP-CCDM ground plane is lowered to contact the DUT pin, then the field plate is brought to the specified charge voltage. At discharge, the reed switch is closed and the current flows up the pogo pin, through a high bandwidth 1Ω resistor, and to ground. The voltage is measured across the 1Ω resistor from which the discharge current waveform is then calculated.

B. RP-CCDM Testing Procedure

The RP-CCDM charges the DUT after the pogo-pin has contacted the pin to be tested. This is to ensure failures due to non-measured currents passed through the capacitance between the lower pogo and the ground plane or through the capacitance inside the reed switch, like the currents observed in [6][7], do not occur when the non-charged pogo tip touches the DUT. By contacting the pin of the DUT first, the potential of the lower portion of the pogo-pin is slowly increased concurrently with the potential of the device. Thus, no high frequency transient can pass through the capacitances as might occur if the neutral pogo tip touched a higher potential pin on the DUT. The single and double discharge methods specified in the JS-002 standard can still be used for pulsing in the RP-CCDM depending on when the discharge relay is closed. The process for the single discharge method, which was used for all tests in this work, is as follows:

Single Discharge Method

1) Test starts with reed switch open; field plate grounded
2) Descend and touch DUT
3) Switch field plate relay to HV at specified TC voltage x voltage ratio
4) Wait for DUT to charge
5) Close reed switch, measure the CDM current
6) Switch field plate to ground
7) Open reed switch
8) Rise and move to next pin

C. Reed Switch

The reed switch used in the pogo pin structure was chosen specifically for its small form factor. The switch was soldered directly to the center of the 1Ω current sensing resistor. A small 3mm pogo pin was soldered directly to the bottom lead of the reed switch to keep the length of the pogo structure as small as possible such that the inductance of the structure would not increase drastically. To analyze the impact the new structure would have on the capacitance and inductance of the RLC discharge circuit, a Z_{DUT} measurement was taken of the system. This measurement setup can be seen in Figure 3. The outer rim of a SMA connector was soldered into a cutout on the center of a copper plated FR4 sheet, which is much larger than the CDM head ground plane, approximately 30 cm x 20 cm, and connected to Port 1 of the VNA. The CDM head to be analyzed was attached to Port 2. The pogo pin of the CDM head was placed on the center pin of the Port 1 SMA with the ground planes parallel and the S11 measurement was extracted from which the Z_{DUT} was extracted. Figure 4 shows the Z_{DUT} measurements of a standard FICDM and the RP-CCDM discharge heads. The measurement displays three clear regions where each of the components in the circuit dominate. The

first positive slope represents the frequency range where the inductance of the VNA ground loop dominates, the negative sloping region represents where the capacitance between the plates dominates, and the third region represents where the inductance of the pogo structure dominates [8].

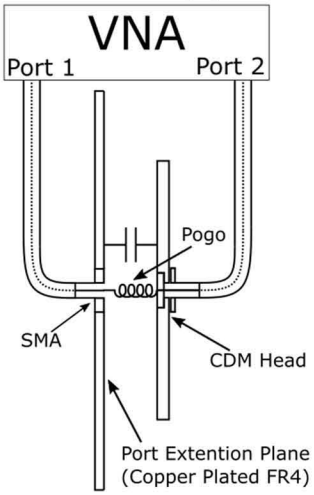

Figure 3: Z_{DUT} Measurement Setup Diagram

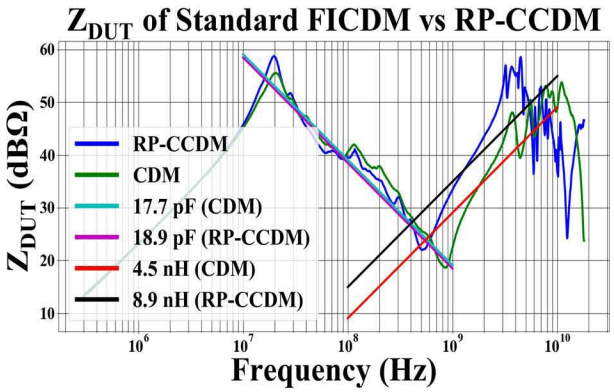

Figure 4: Z_{DUT} Measurement Results

The values of the capacitance between the plates and the inductance of the pogo structure were estimated by fitting the impedance curves of capacitance and inductance values to the Z_{DUT} measurement. This was done by finding a linear best fit line between the peak and trough of the Z_{DUT} and matching the capacitance or inductance value to the center frequency of the best fit line. The fitted lines provide rough estimates but allow for a general assessment of the differences between the discharge heads. This method yielded a significant increase in the inductance from approximately 4.5nH in the CDM pogo structure to approximately 8.9nH in the RP-CCDM pogo structure. Little difference was noted between the capacitance created by the RP-CCDM and standard FICDM head.

D. Charge Stored in the Pogo Tip

The tip of the RP-CCDM pogo structure is electrically isolated from the upper portion of the structure and the ground plane. As a result, there is a small charge that is stored in the tip when the DUT is charged. When the relay is closed the small amount of charge travels through the 1Ω current measurement resistor with the true stress current. To measure the extent to which this would be a factor in the discharge, the large verification module was charged at a field plate voltage of 500V with the pogo touching. After the module was fully charged, the head was raised up and the relay was closed. Figure 5 shows the discharge waveform measured from repeating this procedure ten times compared with the discharge from a JS-002 small verification module. The current measured is most likely negligible if the DUT is large. However, this could be of significance when testing a small DUT since the current produced from this extra charge is independent of DUT size. The possible effect on failure levels of small devices has not yet been evaluated.

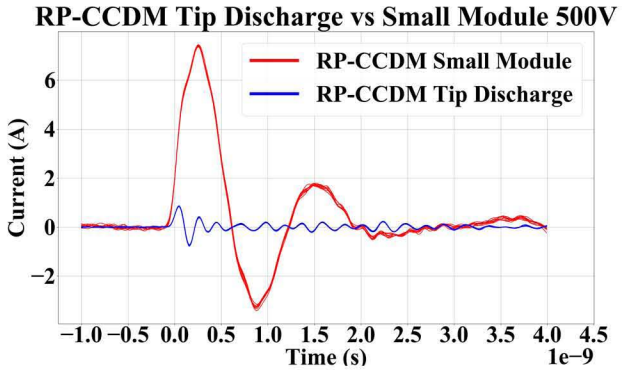

Figure 5: 10 Discharges of Charge Stored in RP-CCDM Pogo Tip 500V

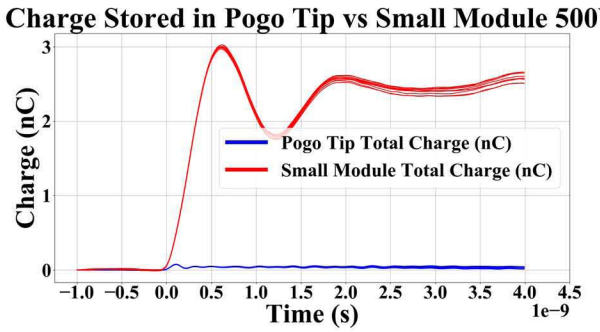

Figure 6: Integration of Small Verification Module and Pogo Tip Discharge Waveforms

The charge transferred during one discharge of the tip was compared to the charge transferred during one discharge of the small JS-002 module as a reference of the impact the additional charge could have, this is

shown in Figure 6. Over 10 pulses the average charge transferred in a discharge of the pogo tip was 0.029 nC, whereas the charge transferred in a discharge of the small module was 2.593 nC on average. Thus, the charge stored in the tip represents approximately 1.14% of charge discharged from small verification module.

III. RP-CCDM vs FICDM Discharge Characteristics

A. Comparison of Standard Test Conditions

To test the discharge characteristics produced by the RP-CCDM head, it was tested using the small and large verification modules defined by the JS-002 standard [2]. The comparison data was collected using a standard FICDM head, also manufactured by ESDEMC Technology. The modules and pogo tips were cleaned with isopropyl alcohol before testing as well as the field plate dielectric surface. The humidity of the test environment was lowered to below 10% RH during testing of the standard FICDM head using a desiccant and compressed air system. As per the JS-002 standard a voltage factor was used to correlate the charge voltage with the desired discharge current. The voltage factor used for the RP-CCDM was 1.08 and the voltage factor for the standard FICDM was 1.02. The true 1Ω current measurement resistor values were 1.026 and 1.030 for the standard FICDM and RP-CCDM heads, respectively. All waveforms were measured using a 6GHz Bandwidth Oscilloscope.

Table 1: Standard Test Level Comparison Measurements

	Small Module		Large Module	
Tester	RP-CCDM	FICDM	RP-CCDM	FICDM
%RH	23%	5%	23%	5%
Ip avg(A)	7.51	7.87	10.68	11.2
Tr avg(ps)	220	177	260	223
Td avg(ps)	429	339	720	495
Ip2(%Ip1)	44.20%	48.80%	13.50%	23.80%

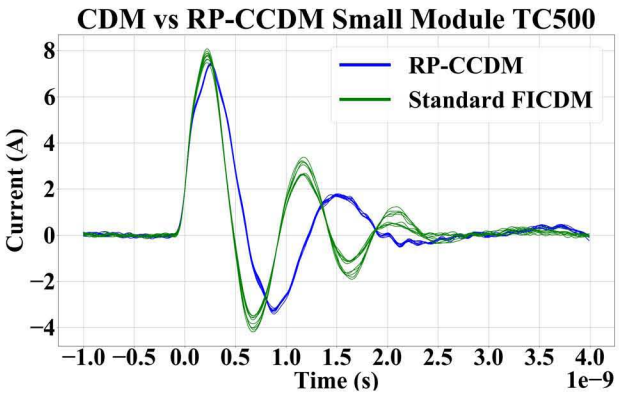

Figure 7: Small Module Comparison of TC500

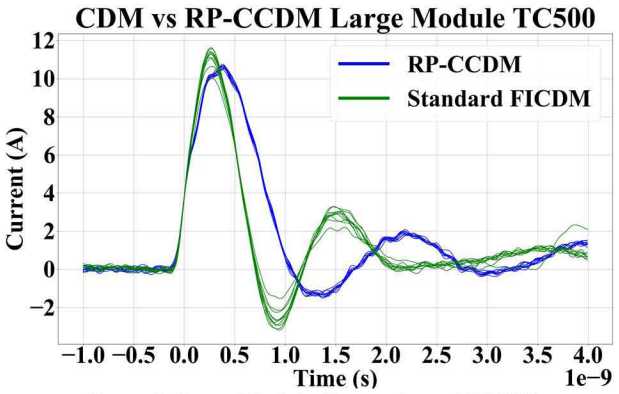

Figure 8: Large Module Comparison of TC500

A full test of both setups verified that they complied with the JS-002 standard measurements. The pulse width of the RP-CCDM was considerably longer than that of the standard FICDM head, especially with the larger module. This can be attributed to the increased inductance of the pogo pin. However, the RP-CCDM head easily fits into the pulse width specification in the JS-002 standard. Some distortion in the peak area is also seen across both modules. It is not clear yet whether this distortion has any impact on the failure levels of devices.

B. Linearity of Discharge Current

The main advantage of the RP-CCDM is the ability to produce a repeatable discharge inside of the reed switch portion of the pogo pin. Figures 9 and 10 were created by normalizing the current and voltage relationship of the TC125 test to 1, for both the standard FICDM and the RP-CCDM. A value of 1 represents a perfectly linear relationship. The highlighted region around the centerline represents where the highest and lowest pulses fell at each test level. To illustrate the repeatability benefits.

Table 2: Small Module Variation Data

Test	Tester	Max variation above mean (%Ip)	Min variation above mean (%Ip)
TC125	RP-CCDM	5.2%	-1.0%
	FICDM	5.1%	-5.8%
TC250	RP-CCDM	1.8%	-2.5%
	FICDM	2.6%	-2.3%
TC500	RP-CCDM	0.3%	-0.5%
	FICDM	3.6%	-3.9%
TC750	RP-CCDM	3.5%	-0.9%
	FICDM	9.8%	-11.0%
TC1000	RP-CCDM	3.5%	-2.0%
	FICDM	3.5%	-5.8%

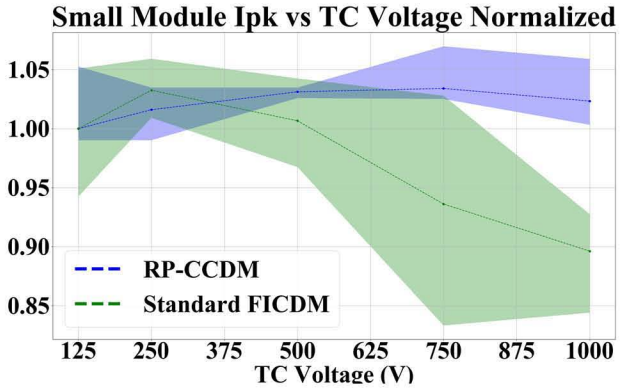

Figure 9: Small Module Linearity and variation plot

Table 3: Large Module Verification Data

Test	Tester	Max variation above mean (%Ip)	Min variation above mean (%Ip)
TC125	RP-CCDM	5.6%	-1.7%
	FICDM	8.4%	-9.1%
TC250	RP-CCDM	2.4%	-3.6%
	FICDM	2.2%	-2.2%
TC500	RP-CCDM	1.2%	-1.6%
	FICDM	4.7%	-10.1%
TC750	RP-CCDM	1.8%	-0.6%
	FICDM	5.5%	-10.2%
TC1000	RP-CCDM	3.2%	-3.6%
	FICDM	6.7%	-6.5%

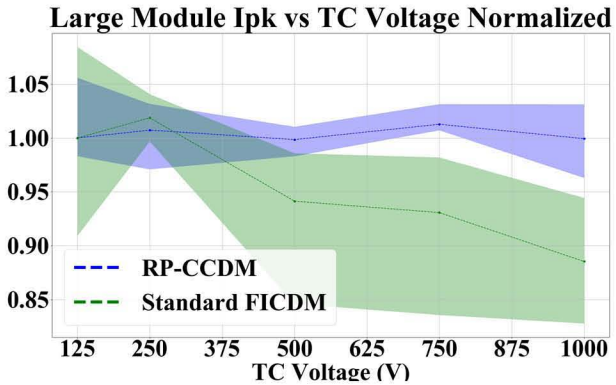

Figure 10: Large Module Linearity and Variation Plot

In addition to a more repeatable discharge, Figures 7 and 8 show the RP-CCDM is also able to produce a peak current that is more linear with respect to increasing voltage. The much lower pulse to pulse variation of the RP-CCDM would make it easier to standardize the failure levels of devices, which has been a large issue with standard FICDM testing [1].

C. Low Voltage Performance

Since the peak current variation is less in RP-CCDM configuration, this will provide better repeatability at low voltage levels. Table 4 and Figure 11 show the results of 100 discharges performed with a field plate charge voltage of 75V using the JS-002 small verification module for both the standard FICDM head and the RP-CCDM head.

Table 4: 75V, 100 Pulse Small Module Test Variability

Tester	Ip Avg (A)	Max variation above mean (%Ip)	Max variation below mean (%Ip)
RP-CCDM	1.04	3.4%	-2.2%
FICDM	1.03	23.8%	-27.0%

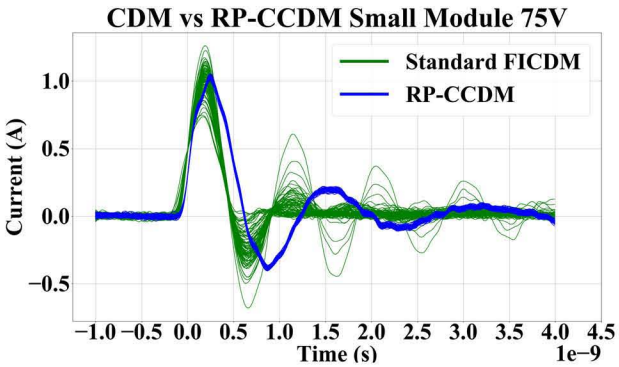

Figure 11: 100 pulse test at charge voltage 75V

As shown in Figure 12, the RP-CCDM can produce repeatable pulses within a +/- 5% window of the peak current even at voltages well below the lowest test condition used for classification.

Further, the RP-CCDM was tested at lower voltages to find where it could no longer produce repeatable pulses (at these voltages the standard FICDM was too unstable to trigger properly). The RP-CCDM tests were run in two ways: first, with the pogo pin sitting on the small verification module, charging and discharging without moving, and second, with the standard single discharge procedure. These results, tabulated and shown in Table 5 and Figure 12, showed that the pulse was less repeatable when the pogo pin re-contacted the disk every pulse. This difference is most likely due to small differences in contact resistance between pulses and highlights the impact contact resistance can have at very low voltages.

Table 5: 25V, 100 Pulse Small Module Test Variability

RP-CCDM Tester Setup	Ip Avg (A)	Max variation above mean (%Ip)	Max variation below mean (%Ip)
Stationary	0.35	3.14%	-13.14%
Moving	0.35	5.84%	-22.53%

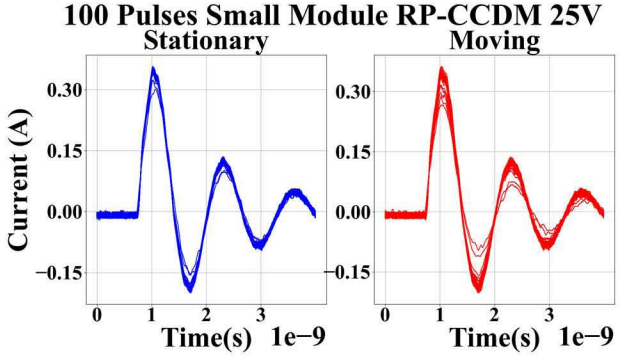

Figure 12: 100 pulse tests at 25V. The stationary test (left) was run with the pogo pin sitting on the module, charging and discharging without moving. The moving test (right) was run with the standard single discharge procedure.

At 10V, over the course of 100 pulses there were many extraneous pulses for both stationary and moving tests, likely making the RP-CCDM pulse unclassifiable at this level. These results are tabulated and shown in Table 6 and Figure 13.

Table 6: 75V, 100 Pulse Small Module Test Variability

RP-CCDM Tester Setup	Ip Avg (A)	Max variation above mean (%Ip)	Max variation below mean (%Ip)
Stationary	.13	6.13%	-33.67%
Moving	.13	22.68%	-27.57%

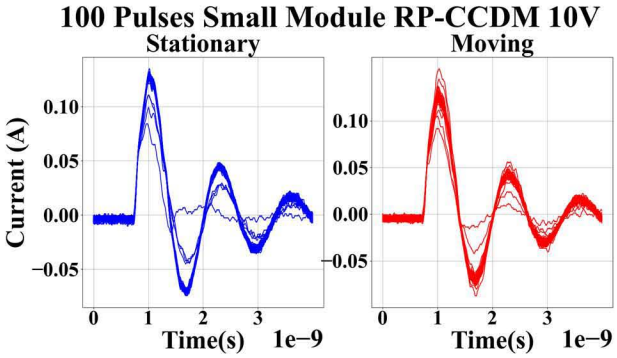

Figure 13: 100 pulse tests at 25V. The stationary test (left) was run with the pogo pin sitting on the module, charging and discharging without moving. The moving test (right) was run with the standard single discharge procedure.

IV. Device Failure Analysis

Test ICs were used to investigate the failure correlation between the standard FICDM and the RP-CCDM test setups. Pre-charging voltage values are 500 V, 625 V and 750 V, while two devices are tested per each method using three discharges per polarity. The chip offers several power and IO domains that are all stressed either in the FICDM test or RP-CCDM test, respectively.

The device failure analysis of the correlation study between FICDM and RP-CCDM is carried out via IDDQ testing. The failure is expected for pre-charging voltages higher than 500 V and located on the edge of the digital core. The IDDQ analysis measures the current consumption in the quiescent state on 200 vectors in the digital core.

The quiescent current into VDD for all vectors is below 100 μA, in case of an unstressed reference device. Slight deviations in this range are traced back to normal variations. A significant increase of the current compared to the reference device indicates a gate-oxide failure on the edge of the digital core.

The device stressed at 500V using FICDM method shows a current consumption below 100 μA, indicating the device can withstand the stress. The device stressed at 625 V using FICDM method, shows an increased current consumption up to 180 μA, which indicates a failure. The failure analysis of the devices stressed at

500V using RP-CCDM method, showed an increased current consumption between 210 µA and 250 µA, indicating failures. The device stressed using RP-CCDM method at 625 V, the measured current level is higher compared to the reference, and higher than the IDDQ values of the devices tested at 500 V using RP-CCDM method. Both failure analysis results for RP-CCDM method are interpreted as a device failure.

By comparing the IDDQ measurements for the failing devices, analyses show a very similar change for the same vectors. This is a strong indication that both test methods trigger the same failure mechanism. In order to get a deeper understanding of the failure mechanism and find out the pass level, a new device is tested with RP-CCDM at 400 V. The IDDQ analysis shows that the device can withstand this stress level. The IDDQ analysis is shown in Figure 14.

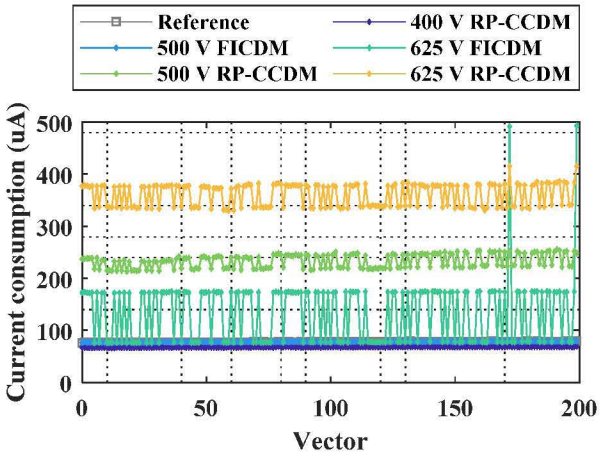

Figure 14: IDDQ analysis for stressed devices with different methods and pre-charging voltage. A current consumption below 100 µA indicates a pass device.

The discharge waveforms of a sensitive IO pin are plotted for FICDM and RP-CCDM in Figure 15 and Figure 16, respectively. FICDM waveforms are recorded with 23 GHz bandwidth, RP-CCDM waveforms with 12 GHz bandwidth (different bandwidth is simply due to the RP-CCDM test being run at a later date with a different oscilloscope). The discharge waveforms are symmetric regarding the polarity, therefore, for simplification, only the positive waveforms are plotted. By comparing the peak currents of the discharges on the IO pin, a dependency of the failure level on the peak current can be determined. The peak currents of each stress corresponding to the shown waveforms are listed in Table 7. The IDDQ analysis and the peak current values lead to the conclusion that the failure is triggered from exceeding the maximum peak current the device can withstand. According to the peak current values, the failure threshold is located between 4.1 A and 4.7 A.

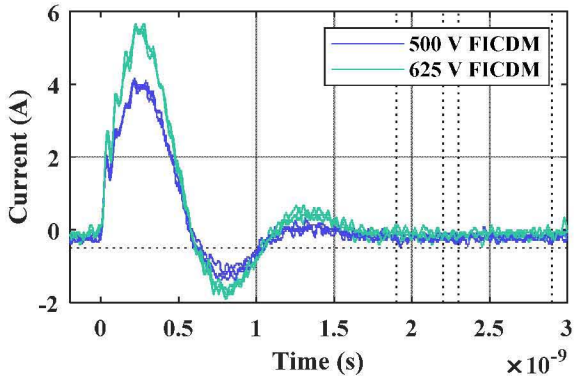

Figure 15: FICDM discharge waveforms for 500 V and 625 V pre-charging voltage.

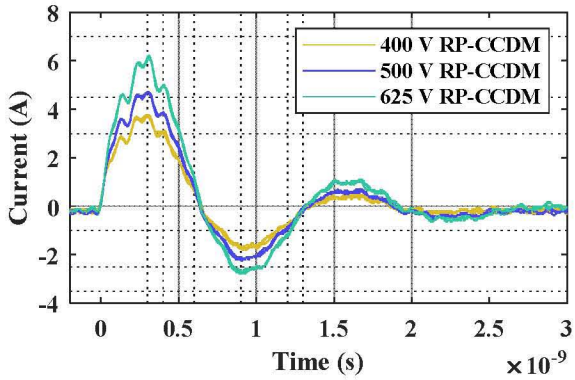

Figure 16: RP-CCDM waveforms for pre-charging voltages of 400 V, 500 V and 625 V.

Table 7: Peak current values for both testing methods and different pre-charging voltages.

Voltage	I_{peak}[CDM]	I_{peak}[RP-CCDM]
400 V	-	3.8 A
500 V	4.1 A	4.7 A
625 V	5.6 A	6.1 A

The failures are reproducible for all tests with a statistic of four devices each, while all pins of the device are stressed.

Even if the waveforms for RP-CCDM are characterized by a longer pulse width and a slightly increased peak current, the total exchanged charge during the discharge event does not offer a significant difference between the different pins and testing methods. This is visualized with a box plot for twelve positive discharges on two devices and various pins in Figure 17. Further, the box plot shows that the RP-CCDM method produces less variation.

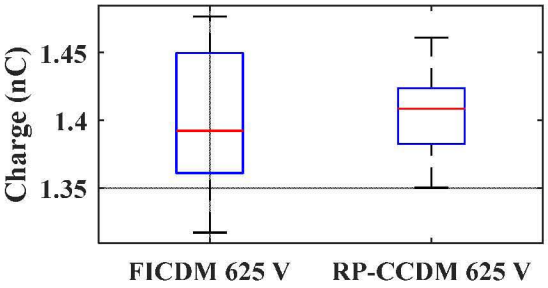

Figure 17: Box plot for the calculated charge during the discharges using FICDM and RP-CCDM at 625 V.

The EMMI scan for a failing FICDM and RP-CCDM device indicate that the spot of the failure is located in the core at the same place, meaning both methods trigger the same failure mechanism. Pictures of the failure signature are shown in Figure 18.

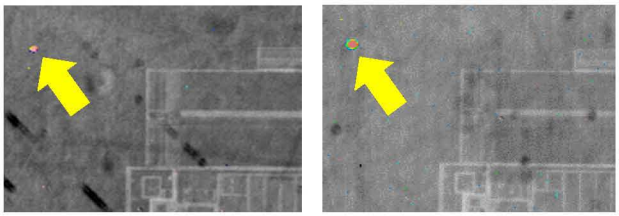
Figure 18: EMMI scan for a failing device tested with FICDM (left) and RP-CCDM (right). Both scans show the same failure location.

The failure level is further investigated by using Capacitively Coupled TLP (CC-TLP). This method allows correlating peak current levels or different pulse width settings to CDM stress parameters and can be applied to investigate CDM type failure modes [7, 9]. For the test device used in this study, the failure can be reproduced at about 5 A, using CC-TLP. FICDM and RP-CCDM failure levels are slightly different concerning the pre-charging voltage, but the CC-TLP test result supports that the failure mechanism is the excess of a certain peak current value.

The increased peak current of the RP-CCDM compared to the standard FICDM test could be adjusted with the test condition according to JS-002 in the future. RP-CCDM waveforms are very stable and the variation between several discharges is negligible, which is a benefit compared to FICDM.

Variations between standard FICDM discharges can be referred to the statistical influence of the spark that again varies with multiple parameters, such as the charging voltage or physical dimensions of package pins or balls. The spark limits the peak current and the oscillation, because of the resistive characteristic, which is considered as a series resistor and inductor in a circuit simulation [8]. Further, a slightly higher effective device capacitance could be assumed in the case of the RP-CCDM test, since the pogo pin is already touching the device before the discharge. This increase in capacitance is due to the fact that field plate and ground plate are closer together. The interaction between the device capacitance and tester capacitances are material for further investigations, including the altered resistance and inductance relationships.

V. Conclusion and Further Investigations

The RP-CCDM demonstrates that it can produce CDM pulses that closely match the pulses produced by a standard FICDM head within the testing framework of the JS-002 standard. However, device failure levels produced by the RP-CCDM head did not directly correlate to failure levels produced by the standard FICDM head. In the case study, the gap between failure levels at 500 V and 625 V can be referred to as a slightly higher peak current in the case of the RP-CCDM waveforms. Further investigations into the current that could flow from the capacitance between the pogo pin and the ground plane or within the reed switch when the uncharged pogo tip contacts a charged DUT are needed. Full-wave simulations of the RP-CCDM system are planned in order to better understand the effects any unmeasured currents may have on the test results.

VI. Acknowledgements

We would like to thank Dr. Kai Esmark from Infineon Technologies AG for providing the testing devices, for his support regarding the failure analysis and for sharing his wide knowledge of ESD, and in particular, of CDM.

VII. References

1. Industry Council on ESD Target Levels, "White Paper 2: A Case for Lowering Component Level CDM ESD Specifications and Requirements," Rev 2, April 2010.
2. ANSI/JEDEC/ESDA, "Joint Standard for Electrostatic Discharge Sensitivity Testing – Charged Device Model," JS-002, 2018.
3. R. Given, M. Hernandez, and T. Meuse, "CDM2 – A New CDM Test Method for Improved Test Repeatability and Reproducibility," in *Proc. EOS/ESD Symp.*, 2010, pp. 359-367.
4. N. Jack, E. Rosenbaum, "Comparison of FICDM and Wafer-Level CDM Test Methods," IEEE

Transactions on Device and Material, vol. 13 no. 2, pp. 379-387, June 2013.

5. Patent Pending
6. D. Johnsson, K. Domanski, and H. Gossner, "Device Failure from the Initial Current Step of a CDM Discharge," in *Proc. EOS/ESD Symp.*, 2018, Paper 6A.4.
7. J. Weber, R. Fung, R. Wong, H. Wolf, H. Geiser, L. Maurer, "Comparison of CDM and CC-TLP Robustness for an Ultra-High-Speed Interface IC," in *Proc. EOS/ESD Symp.*, 2018, Paper 6A.1.
8. F. zur Nieden, K. Esmark, S. Seidl and R. Gärtner, "Predict the product specific CDM stress using measurement-based models of CDM discharge heads," 2016 38th Electrical Overstress/Electrostatic Discharge Symposium (EOS/ESD), Garden Grove, CA, 2016
9. L. Zeitlhoefler, F. zur Nieden, K. Esmark, G. Langguth and F. Kreupl, "Energy of CDM Failure for ICs on Package-, Wafer-and Board-Level," 2019 41st Annual EOS/ESD Symposium (EOS/ESD), Riverside, CA, USA, 2019